

Bright narrowband source of photon pairs at optical telecommunication wavelengths using a type-II periodically poled lithium niobate waveguide

Go Fujii¹, Naoto Namekata^{1*}, Masayuki Motoya¹, Sunao Kurimura², and Shuichiro Inoue¹

¹*Institute of Quantum Science, Nihon University, 1-8-14 Kanda-Surugadai, Chiyoda-ku, Tokyo 101-8303, Japan*

²*National Institute for Materials Science, 1-1 Namiki, Tsukuba-shi, Ibaraki 305-0044, Japan*

[*mnao@phys.cst.nihon-u.ac.jp](mailto:mnao@phys.cst.nihon-u.ac.jp)

Abstract: We report on the generation of narrowband photon pairs at telecommunication wavelengths using a periodically poled lithium niobate waveguide that utilizes the nonlinear tensor element d_{24} for type-II quasi phase matching. The FWHM bandwidth of the spontaneous parametric downconversion was 1 nm. The brightness of the photon pair source was $\sim 6 \times 10^5$ /s/GHz when the pump power was 1 mW. The indistinguishability of the signal and idler photons generated by the degenerate spontaneous parametric downconversion process was studied in a Hong-Ou-Mandel type interference experiment.

© 2007 Optical Society of America

OCIS codes: (270.0270) Quantum optics; (190.4410) Nonlinear optics.

References and links

1. N. Gisin, G. Ribordy, W. Tittel, and H. Zbinden, "Quantum cryptography," *Rev. Mod. Phys.* **74**, 145-195 (2002).
2. J. W. Pan, D. Bouwmeester, H. Weinfurter, and A. Zeilinger, "Experimental nonlocality proof of quantum teleportation and entanglement swapping," *Phys. Rev. Lett.* **88**, 017903.1-017903.4 (1998).
3. D. Bouwmeester, J. W. Pan, K. Mattele, M. Eibl, H. Weinfurter, and A. Zeilinger, "Experimental quantum teleportation," *Nature* **390**, 575-579 (1997).
4. P. G. Kwiat, K. Mattele, H. Weinfurter, A. Zeilinger, A. V. Sergienko, and Y. Shih, "New high-intensity source of polarization-entangled photon pairs," *Phys. Rev. Lett.* **75**, 4337-4341 (1995).
5. A. Yoshizawa, R. Kaji and H. Tsuchida, "Two-photon interference at 1550nm using two periodically poled lithium niobate waveguides," *Jpn. J. Appl. Phys.* **42**, 5652-5653 (2003).
6. H. de Riedmatten, I. Marcikic, W. Tittel, H. Zbinden and N. Gisin, "Quantum interference with photon pairs created in spatially separated source," *Phys. Rev. A.* **67**, 022301.1-022301.5 (2003).
7. C. K. Hong, Z. Y. Ou and L. Mandel, "Measurement of subpicosecond time intervals between two photons by interference," *Phys. Rev. Lett.* **59**, 2044-2046 (1987).
8. H. Y. Shen, H. Xu, Z. D. Zeng, W. X. Lin, R. F. Wu, and G. F. Xu, "Measurement of refractive indices and thermal refractive-index coefficients of LiNbO₃ crystal doped with 5 mol.%MgO," *Appl. Opt.* **31**, 6695-6697 (1992).
9. T. Suhara, and H. Kintaka, "Quantum theory analysis of twin-photon beams generated by parametric fluorescence," *IEEE Quantum Electron.* **41**, 1203-1205 (2005).
10. M. Motoya, S. Kurimura, S. Inoue, Y. Usui and H. Nakajima, "Type II quasi-phase matching in waveguide parametric down converter for quantum information technologies," *Conference on Lasers and ElectroOptics*, Long Beach, USA (2006), CMB5.
11. N. Namekata, Y. Makino and S. Inoue, "Single-photon detector for long-distance fiber-optic quantum key distribution," *Opt. Lett.* **27**, 954-956 (2002).

12. S. Mori, J. Söderholm, N. Namekata and S. Inoue, "On the distribution of 1550-nm photon pairs efficiently generated using a periodically poled lithium niobate waveguide," *Opt. Com.* **264**, 156-162 (2006).
13. H. de Riedmatten, V. Scarani, I. Marcikic, A. Acín, W. Tittel, H. Zbinden and N. Gisin, "Two independent photon pairs versus four-photon entangled states in parametric down conversion," *J. Mod. Opt.* **51**, 1637-1649 (2004).
14. C. Langrock, E. Diamanti, R. V. Roussev, Y. Yamamoto, M. M. Fejer, and H. Takesue "Highly efficient single-photon detection at communication wavelengths by use of upconversion in reverse-proton-exchanged periodically poled LiNb3 waveguide," *Opt. Lett.* **30**, 1725, (2005)
15. R. H. Hadfield, J. L. Habif, J. Schlafer, R. E. Schwall, and S. W. Nam, "Quantum key distribution at 1550 nm with twin superconducting single-photon detector," *Appl. Phys. Lett.* **89**, 241129.1-241129.3 (2006)

1. Introduction

Photon pairs in the telecommunication band are an essential resource for practical quantum communication systems such as quantum key distribution[1], entanglement swapping[2] and quantum teleportation[3]. The photon pairs can be easily generated by the spontaneous parametric down conversion (SPDC) in a second-order nonlinear crystal[4]. Using a periodically poled lithium niobate (PPLN) waveguide, we can generate photon pairs in telecommunication band efficiently because of the long interaction length and the strong confinement of a pump energy. The PPLN waveguide utilizes the nonlinear tensor element d_{33} for the type-0 quasi-phase matching (QPM) in which copolarized photon pairs are generated. Since the element d_{33} has the higher nonlinear coefficient than any other elements, the type-0 PPLN waveguide has the highest conversion efficiency[5]. However, in application to the entanglement-based quantum communication, a broad spectral width (\sim THz) of the type-0 photon pairs limits the fiber transmission distance. As regards the time-bin entanglement, a chromatic dispersion (\sim 10 ps/km/nm, in standard single-mode fibers) degrades a purity of the entanglement. To realize sharing the entangled photons over long distance ($>$ 100 km: standard fiber), the spectral width should be less than \sim 0.1 nm. Although the condition can be obtained using a narrow band pass filter, the generation rate of the photon pairs (unit: pairs/s) is significantly reduced by the filtering. Therefore, the photon pair sources should be evaluated by the generation rate normalized to the bandwidth, namely the brightness (unit: pairs/s/GHz). And consequently, a photon pair source with a high brightness is required for the long-distance quantum communication.

In this paper, we report on the generation of narrowband photon pairs at telecommunication wavelengths using a PPLN waveguide utilizing the nonlinear tensor element d_{24} for the type-I QPM. We have demonstrated that the brightness of the photon pair source is higher than that of a conventional type-0 photon pair source (a proton-exchanged PPLN waveguide). Furthermore, the type-II PPLN generates crosspolarized photon pairs that can be efficiently split into two different spatial modes even if the photon pairs are generated by the degenerate SPDC process. This indicates that an optical loss in a transmission fiber can be minimized by setting the wavelengths of both of the signal and idler photons to 1550 nm (C-band). Finally, in order to investigate the indistinguishability of the signal- and idler- photons, we performed a Hong-Ou-Mandel (HOM) type interference experiment [7].

2. Narrowband photon pairs

First of all, let us consider the SPDC process in a periodically poled nonlinear waveguide. We assume that the pump beam (wavelength λ_3 , frequency ω_3) is coupled into the nonlinear waveguide, then the photon pairs (λ_1, ω_1 : idler photon and λ_2, ω_2 : signal photon) are generated by the SPDC process. The relation between the three wavelengths is

$$\frac{1}{\lambda_3} = \frac{1}{\lambda_1} + \frac{1}{\lambda_2}. \quad (1)$$

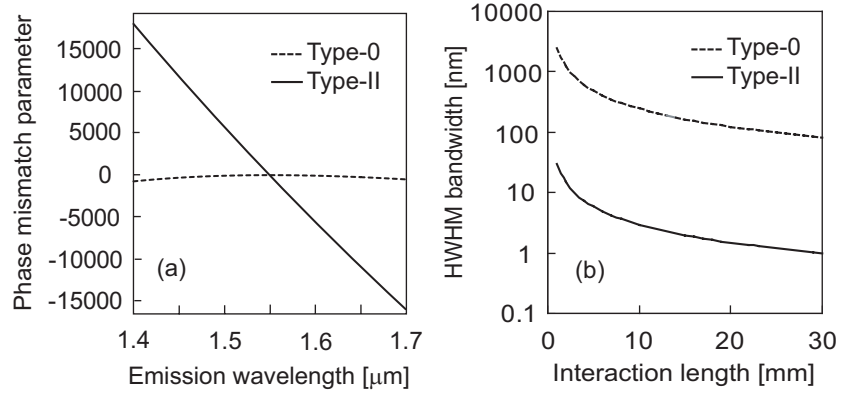


Fig. 1. Comparisons between the SPDC bandwidths of type-0 and type-II QPM devices. The dashed and solid lines show the numerical results using Eqs. (1) ~ (3). (a) the phase mismatch parameters as functions of the pump wavelength. (b) the SPDC bandwidths as functions of the interaction length.

The QPM condition is expressed as

$$\Delta = \pi \left[\frac{n_3}{\lambda_3} - \left(\frac{n_1}{\lambda_1} + \frac{n_2}{\lambda_2} + \frac{1}{\Lambda} \right) \right], \quad (2)$$

where n_k is the refractive index at λ_k , Δ is the phase-mismatch parameter, and Λ is the QPM grating period. In the case of the type-0 QPM, $n_{1,2,3}$ are the ordinary refractive indices of the bulk LiNbO₃ crystal [8]. On the other hand, in the case of the type-II QPM, $n_{1,3}$ and n_2 are the ordinary and extraordinary refractive indices, respectively. The QPM grating period is determined by $\Delta = 0$. The power of the SPDC outputs from the nonlinear waveguide is then given by the expression [9]:

$$P \propto \omega_1 \int \left| \frac{\sinh(l \sqrt{(\omega_1/\omega_2) \kappa^2 P_3 - \Delta^2})}{l \sqrt{(\omega_1/\omega_2) \kappa^2 P_3 - \Delta^2}} \right|^2 d\omega_2, \quad (3)$$

where l is the interaction length, κ is the nonlinear coupling coefficient, and P_3 is the input pump power. In Fig. 1(a), the phase-mismatch-parameter of the type-II and type-0 QPM devices are shown as functions of the emission wavelength. When the degenerate wavelength was 1550 nm, Λ for the type-0 and type-II QPM were 19 μm and 9 μm, respectively. In the case of the type-0 QPM, Δ gently varies with changing the emission wavelength. On the other hand, in the case of the type-II QPM device, Δ is significantly changed, which is due to the difference of the refractive indices for the signal and idler photons. This suggests that the SPDC bandwidth of the type-II QPM device is much narrower than that of the type-0 QPM device, because the SPDC can occur at a neighborhood of $\Delta = 0$. Figure 1(b) shows the interaction-length dependence of the SPDC bandwidth that is the full width at half maximum (HWHM) of the power spectrum evaluated from Eq. (3). As the interaction length is longer, the SPDC bandwidth becomes narrower. As shown in Fig. 1(b), the 30-mm-long type-II QPM device can realize a SPDC bandwidth of ~1 nm.

3. Experimental setup

Our experimental setup is schematically depicted in Fig. 2. A pump beam was injected into a 30-mm-long adhered ridge waveguide of the type-II PPLN.[10] The waveguide in the squared shape was formed by a dry etching technique. The height and width of the waveguide were $3.0\ \mu\text{m}$ and $6.0\ \mu\text{m}$, respectively. The ridge waveguide allows a strong confinement of the pump energy and an efficient transmission of light in both the TE and TM mode. The CW external cavity diode laser (Toptica Photonics DLX110) was used for the pump source whose wavelength was $777\ \text{nm}$ with a linewidth of $1\ \text{MHz}$. The degenerate photon pairs at $1554\ \text{nm}$ were generated when the QPM grating period was $8.1\ \mu\text{m}$ and the device temperature was stabilized at 28.8°C (The degenerate wavelength could be $1550\ \text{nm}$ by setting the device temperature to $\sim 55^\circ\text{C}$, since the temperature dependence of the degenerate wavelength was $-0.15\ \text{nm}/^\circ\text{C}$). The signal (in TM mode) and idler (in TE mode) photons were orthogonally polarized each other. In order to measure only the down-converted photon pairs, the emerging

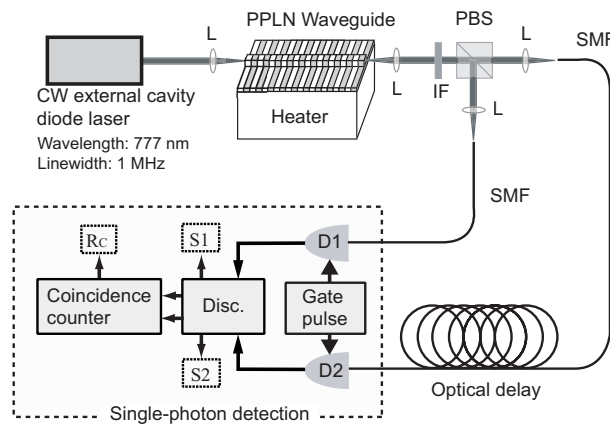


Fig. 2. Experimental setup to measure the generation rate of photon pairs. L: lenses, IF: interference filter, PBS: polarizing beamsplitter, SMF: single-mode fiber, Disc.: Discriminator, D1,2: single-photon detectors, S1,2: single-count rate at D1,2, R_C : coincidence-counts per second.

light from the waveguide passed through an interference filter (IF) centered at $1550\ \text{nm}$ (width of $30\ \text{nm}$). The signal and idler photons were separated by a polarizing beamsplitter (PBS), and subsequently coupled into the single-mode fibers (SMFs) to be led to the single-photon detectors (D1 and D2). The entire optical losses experienced by the downconverted photons impinging upon each detector were $9.2\ \text{dB}$. The detectors are electrically cooled InGaAs/InP avalanche photodiodes (EPITAXX EPM239BA) operated with a short gated mode [11]. The gate duration was $\sim 2\ \text{ns}$ and the repetition frequency of the gate was $500\ \text{kHz}$. The detection efficiency of D1 and D2 were 20% and 19% with the dark-count probability per gate of $4.6 \cdot 10^{-5}$ and $4.8 \cdot 10^{-5}$, respectively.

4. SPDC bandwidth

Figure 3 shows the measured spectrum of the photon pairs generated by the type-II PPLN waveguide. For comparison, the spectrum of the photon pairs generated by the type-0 PPLN waveguide is also shown in the figure. The 30-mm-long proton-exchanged PPLN waveguide (HC photonics) was used as the type-0 QPM device. The spectra were measured by an optical

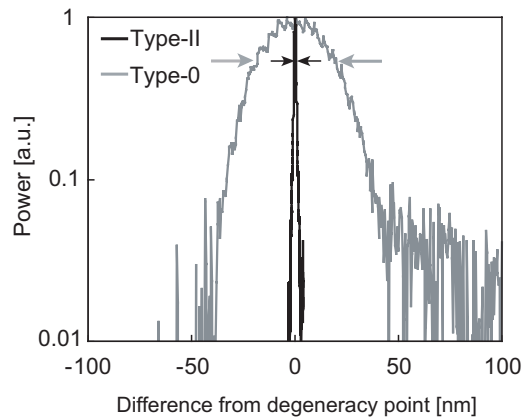


Fig. 3. Comparison between the measured spectra of the photon pairs generated by the two different types of QPM devices. The gray and black lines show the spectra of the photon pairs generated by the type-0 and type-II QPM devices, respectively.

spectrum analyzer whose resolution bandwidth was set to 1.0 nm. The measured bandwidth of the photon pairs generated by the type-0 QPM device was 40 nm (centered at 1551 nm). In contrast, the bandwidth of the photon pairs generated by the type-II PPLN waveguide was only 1 nm (centered at 1554 nm). Here, we must note that the measured value of the bandwidth is very close to the resolution bandwidth of the optical spectrum analyzer. Therefore, the real bandwidth of the SPDC output might be less than 1 nm (the theoretical value is 0.8 nm). The SPDC bandwidth of the type-II PPLN waveguide was 1/40 compared to that of the type-0 PPLN waveguide. The coherence time of the photon pairs was estimated as 3.6 ps. (note that we assumed the transform-limited photon wavepacket) [13]. In contrast, that of the photon pairs generated by the type-0 QPM device was only 0.09 ps.

5. Photon counting results

In Fig. 4, the measured coincidence-count rates are plotted as a function of the single-count rate that is the average count rates for the two detectors. The dark counts is subtracted from the experimental data. The theoretical curve is also shown in the figure. The experimental results were in good agreement with the Poisson-statistics-based theory [12] in which the overall optical losses and detection efficiencies were taken into account. We obtained a single-count rate of $5.1 \times 10^4 \text{ s}^{-1}$ and coincidence-count rate of $6.3 \times 10^3 \text{ s}^{-1}$ when the type-II QPM device was pumped with an average power of 25 mW (coupled into the waveguide). Corrected for the detection efficiencies of SPDs and the optical losses, the generation rate of the crosspolarized photon pairs was $2.3 \times 10^9 \text{ s}^{-1}$. Table 1 shows the comparison of the performances of the photon pair sources. Here, note that the generation rate and the brightness are normalized to a coupled pump power of 1 mW. The brightness of the type-II photon pair source was $\sim 6 \times 10^5 \text{ /s/GHz}$, which was higher than that of the type-0 photon pair source. The type-II SPDC does not cause a large spectral broadening such as the type-0 SPDC. This is the reason why the type-II photon pair source has the higher brightness, even though the nonlinear tensor element d_{24} is smaller than d_{33} .

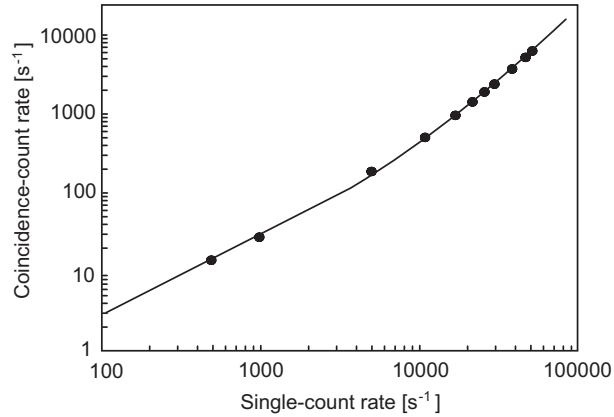


Fig. 4. Experimental and theoretical coincidence-count rates. The filled circles show the measured values of the coincidence-count rates, and the solid line shows the theoretical curve.

Table 1. Measured brightness of the type-0 and type-II QPM devices when the pump power was 1 mW.

QPM type	Bandwidth [nm]	Coherence time [ps]	Generation rate [s ⁻¹]	Brightness [1/s/GHz]
0	40	0.09	1×10^9	$\sim 2 \times 10^5$
II	1	3.6	1×10^8	$\sim 6 \times 10^5$

6. HOM-type interference experiment

Finally, we performed a HOM type interference experiment[7] to investigate the indistinguishability of the signal and idler photons. For generation of the entangled photon pairs, the indistinguishability is very important, since the purity of the entanglement depends upon it. The setup of the HOM type interference experiment is schematically depicted in Fig. 5. The photon pairs (the signal and idler photons) were separated by the PBS, and each photon was led to the different paths and coupled into the slow axis of the polarization maintaining fibers (PMF). Finally they were recombined at a polarization maintaining 50/50 fiber coupler (PMFC). The two outputs of the coupler were connected to the single-photon detectors. The coincidence-count N_c is given by the expression [7]:

$$N_c = C[1 - V_{HOM}e^{(\Delta\omega\delta\tau)^2}], \quad (4)$$

where $\Delta\omega$ is the spectral bandwidth of photon pairs, $\delta\tau$ is a difference between the pass lengths experienced by the signal and idler photons, V_{HOM} is a visibility, C is a normalization constant. In the present experiment, the refractive indices for the TM mode (signal photon) and the TE mode (idler photon) are not the same. Therefore, the optical distances (in the waveguide) experienced by the signal photon is different from that experienced by the idler photon. In addition, the difference between the optical distances is not constant but depends upon a position at which a photon pair is generated in the waveguide. As a result, there exists an uncertainty in the optical path-length difference between the two arms (for the signal and idler photons) of the HOM interferometer. The uncertainty degrades the visibility of the quantum interference. Taking into account the difference between the refractive indices for the TE and TM modes,

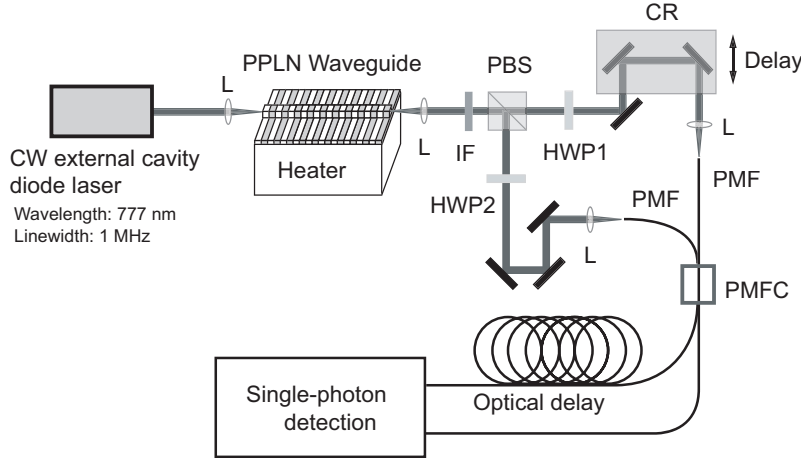


Fig. 5. Schematic diagram of the HOM type interference experiment. HWP1,2; half-wave plate, CR; corner reflector, PMF; polarization maintaining fiber, PMFC; polarization maintaining 50/50 fiber coupler.

Eq. (4) can be rewritten as the simple expression:

$$N_{cd} = C \int_0^{\frac{(n_3+n_2)l}{2c}} \left\{ 1 - \left(\frac{2c}{n_3+n_2} \right) L t_p \right\}^2 \left[1 - e^{\left\{ \Delta\omega \left(\delta\tau - \frac{2(n_3-n_2)}{n_3+n_2} t_p \right) \right\}^2} \right] dt_p, \quad (5)$$

where t_p is a propagation time of the photon pairs and, L is the loss in the waveguide. Figure 6 shows the experimental results when the pump power was 0.5mW. The coincidence count rate in the experiment was lower than that obtained using the setup shown in Fig. 2, which was due to the additional losses (2 dB) of the experimental setup. The figure exhibits the HOM interference dip. The theoretical curve under the experimental conditions ($n_2=2.117$, $n_3=2.196$, $L=0.32$ dB/cm, $\Delta\omega=0.12$ THz) is also plotted in the figure. Here, the n_2 and n_3 were an effective refractive index involving the dimensions of the ridge waveguide. The measured visibility of the HOM interference dip was $\sim 70\%$. In the experiment, an average number of the generated photon pairs in 2 ns gate window was 0.025. In the condition, we can ignore a multiple-photon-pair generation (coincidence between the non-correlated photons) that results in the degradation of the visibility. Therefore, the degradation was caused mainly by the uncertainty in the path-length difference. If we use a 0.2 nm band-pass-filter, the uncertainty will be negligible because the narrowband filtering makes the coherent length longer. Then, the wave packets of the signal and idler photons will practically overlap (visibility $\sim 100\%$). Although, the net generation-rate of the photon pairs will be reduced by the spectral filtering, the normalized generation rate (a pump power of 1 mW) would be still 10^7 s $^{-1}$. This indicates that a bright ultranarrowband photon pair source for telecommunication wavelengths can be realized using the type-II PPLN waveguide.

7. Conclusions

We demonstrated that the type-II PPLN waveguide was able to generate narrowband photon pairs in the telecommunication band efficiently. The bandwidth of the photon pairs was 1 nm which was 1/40 compared to the type-0 QPM device. When the type-II PPLN waveguide was pumped with 25 mW, the generation rate of the crosspolarized photon pairs was 2.3×10^9 s $^{-1}$

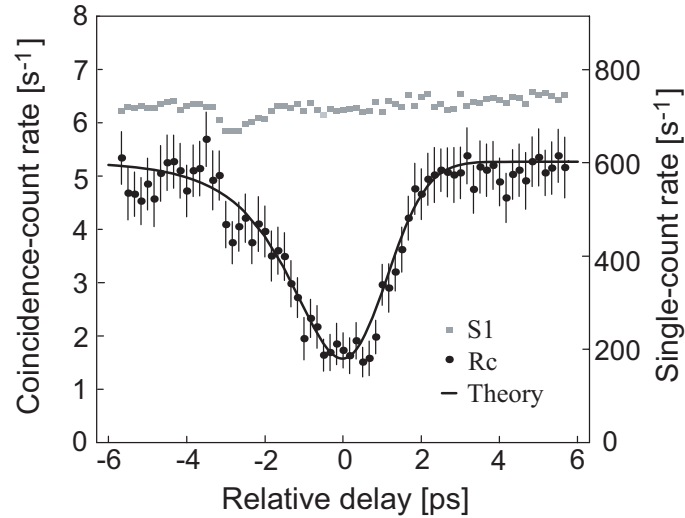


Fig. 6. Experimental results of a Hong-Ou-Mandel type interference experiment. The circles and squares show the measured values of the coincidence-counts and single-counts, respectively as functions of the relative delay between the signal and idler photons. The solid line shows the theoretical curve derived from Eq. (5).

which was corrected for the detection efficiencies of the SPDs and the optical losses. The brightness was $\sim 6 \times 10^5$ /s/GHz when the pump power was 1 mW. Although the nonlinear coefficient d_{24} is smaller than d_{33} , the brightness of the type-II photon pair source was higher than that of the conventional type-0 photon pair source.

The indistinguishability of the signal and idler photons was investigated through the HOM interference experiment. We obtained the interference visibility of $\sim 70\%$. Using a band-pass-filter of 0.2 nm (FWHM), the quantum interference visibility would be further improved to $\sim 100\%$. Moreover, in that condition, the photon pair generation rate is still 10^7 s $^{-1}$.

In our experiment, the gated avalanche photodiodes were used to detect the continuously generated photon pairs. Therefore, the coincidence count rate was very low, although our photon pair source had the high brightness. To increase the coincidence count rate, we should use a single-photon detector operated with a non-gated mode, for example the upconversion detectors[14] and the superconducting single-photon detectors[15]. Moreover, since the coincidence count rate is strongly depends on the optical losses, reduction of the optical losses of the setup (currently: 9.2 dB) is one of the most important issue toward application to the fiber based long-distance quantum key distribution and teleportation system.

Acknowledgments

This work was partly supported by the National Institute of Information and Communications Technology (NICT).